Disruption of the 5S RNP-Mdm2 interaction significantly improves the erythroid defect in a mouse model for Diamond-Blackfan anemia.

Jaako, Pekka; Debnath, Shubhranshu; Olsson, Karin; Zhang, Y; Flygare, Johan; Lindström, M S; Bryder, David; Karlsson, Stefan

Published in:
Leukemia

DOI:
10.1038/leu.2015.128

2015

Disruption of the 5S RNP-Mdm2 interaction significantly improves the erythroid defect in a mouse model for Diamond-Blackfan anemia

Pekka Jaako[1,2], Shubhranshu Debnath[1], Karin Olsson[1], Yanping Zhang[3], Johan Flygare[1], Mikael S. Lindström[4], David Bryder[2] and Stefan Karlsson[1]

[1]Molecular Medicine and Gene Therapy, Lund Stem Cell Center, Lund University, Lund, Sweden
[2]Molecular Hematology, Lund Stem Cell Center, Lund University, Lund, Sweden
[3]Department of Radiation Oncology, School of Medicine, University of North Carolina at Chapel Hill, Chapel Hill, NC, USA
[4]Department of Oncology-Pathology, Karolinska Institutet, Stockholm, Sweden

Correspondence:
Stefan Karlsson
Molecular Medicine and Gene Therapy, BMC A12, 221 84, Lund, Sweden
Tel: +46 46 222 05 77
Fax: +46 46 222 05 68
Stefan.Karlsson@med.lu.se

Conflict of interest: The authors declare no conflict of interests.

Running title: **5S RNP-Mdm2-p53 pathway in DBA**
Key words: **Diamond-Blackfan anemia, Ribosomal stress, Ribosomal protein, p53**

Abstract: **200 words**
Manuscript: **3965 words**

ABSTRACT

Diamond-Blackfan anemia (DBA) is a congenital erythroid hypoplasia caused by haploinsufficiency of genes encoding ribosomal proteins (RPs). Perturbed ribosome biogenesis in DBA has been shown to induce a p53-mediated ribosomal stress response. However, the mechanisms of p53 activation and its relevance for the erythroid defect remain elusive. Previous studies have indicated that activation of p53 is caused by the inhibition of Mdm2, the main negative regulator of p53, by the 5S ribonucleoprotein particle (RNP). Meanwhile, it is not clear whether this mechanism solely mediates the p53-dependent component found in DBA. To approach this question, we crossed our mouse model for RPS19-deficient DBA with $Mdm2^{C305F}$ knock-in mice that have a disrupted 5S RNP-Mdm2 interaction. Upon induction of the Rps19 deficiency, $Mdm2^{C305F}$ reversed the p53 response and improved expansion of hematopoietic progenitors *in vitro*, and ameliorated the anemia *in vivo*. Unexpectedly, disruption of the 5S RNP-Mdm2 interaction also led to selective defect in erythropoiesis. Our findings highlight the sensitivity of erythroid progenitor cells to aberrations in p53 homeostasis mediated by the 5S RNP-Mdm2 interaction. Finally, we provide evidence indicating that physiological activation of the 5S RNP-Mdm2-p53 pathway may contribute to functional decline of the hematopoietic system in a cell-autonomous manner over time.

INTRODUCTION

Diamond-Blackfan anemia (DBA) is a congenital erythroid hypoplasia characterized by macrocytic anemia with selective absence of erythroid precursors, physical abnormalities, and cancer predisposition[1-3]. DBA is most often caused by mutations in *ribosomal protein S19 (RPS19; eS19)* and other genes encoding ribosomal proteins (RPs)[4-11]. Studies in zebrafish and mouse DBA model systems *in vivo* and human hematopoietic cells *in vitro* have suggested that the anemia is caused by the activation of p53 generated by the

RP deficiency[12-15]. Mice that have a missense mutation in *Rps19* exhibit dark skin, retarded growth and a reduction in the number of erythrocytes, and all of these features are rescued in a p53-null background[12]. Similarly, the lethal hematopoietic phenotype of the transgenic Rps19 knockdown mice is reversed upon loss of p53[15]. Additionally, Dutt *et al*. demonstrated that inhibition of p53 with the small molecule pifithrin alpha rescues the erythroid defect in RPS19-deficient human bone marrow (BM) cell cultures[14].

The identification of p53 as one of the mediators of the DBA phenotype could have therapeutic implications for the treatment of DBA and related disorders. However, strong concerns have to be raised towards therapeutic strategies based on direct interference with p53, given its prominent role as an orchestrator of genetic programs leading to cell cycle arrest, senescence and apoptosis[16]. Therefore, it is important to delineate the components upstream of p53 activation upon RP deficiency as these might provide novel disease-specific targets for therapeutic intervention. The level of p53 is negatively regulated by mouse double minute 2 (Mdm2; HDM2 in humans), which functions as an ubiquitin ligase that targets p53 to the proteasome in the absence of stress[17]. Cellular stress signals, such as DNA damage and oncogenic insults, disrupt the interaction between Mdm2 and p53 resulting in the stabilization and activation of p53[17]. A body of *in vitro* studies indicates that perturbed ribosome biogenesis activates the p53 response through the nuclear accumulation of RPL5 and RPL11 that in turn bind to Mdm2 and inhibit its ubiquitin ligase function toward p53[14,18-20]. More recently, RPL5 and RPL11 were shown to regulate p53 as part of the 5S ribonucleoprotein particle (RNP), in which the 5S ribosomal RNA (rRNA) is also critical for p53 regulation[21,22]. Finally, the physiological relevance of the 5S RNP-Mdm2 interaction was further confirmed by the generation of $Mdm2^{C305F}$ knock-in mice that harbor a missense mutation in the zinc finger region of Mdm2 preventing its binding to 5S RNP[23,24]. Disruption of the 5S RNP-Mdm2 interaction in these mice attenuated the p53 activation upon chemically induced ribosome biogenesis stress, and shortened the latency of c-Myc driven tumorigenesis[23]. However, the physiological relevance of the 5S RNP-Mdm2-p53

pathway for generation of the erythroid defect of DBA is not known. By intercrossing Rps19-deficient mice[15] with the Mdm2^{C305F} knock-in mice[23], we show in the current study that the 5S RNP-Mdm2 interaction has a dominant role in mediating the p53 activation upon Rps19 deficiency and its disruption partially improves the erythropoiesis of Rps19-deficient mice *in vivo*. We also report the unexpected finding that the loss of 5S RNP-Mdm2 interaction *per se* causes mild anemia by triggering a p53 signature in erythroid progenitor cells. Finally, our results indicate that disruption of the 5S RNP-Mdm2 interaction has a positive impact on the reconstitution capacity of serially transplanted hematopoietic stem cells (HSCs), suggesting that the 5S RNP-Mdm2-p53 pathway may contribute to the functional decline of the hematopoietic system upon replicative stress.

MATERIAL AND METHODS

Mice

Generation of transgenic Rps19 knockdown mice and the Mdm2^{C305F} knock-in mice has been described earlier[15,23]. Mice were maintained in C57BL/6 background and litter mate controls were used. Rps19 deficiency was induced by administrating doxycycline in the food (Bio-Serv; 200 mg/kg). Mice were maintained at Lund University animal facility and experiments were performed with consent from the Lund University animal ethics committee.

Blood and bone marrow cellularity

Peripheral blood was collected from the tail vein into Microvette tubes (Sarstedt) and analyzed using Sysmex XE-5000 and Sysmex KX-21 hematology analyzers. BM cells were isolated by crushing hip bones, femurs and tibiae in PBS containing 2 % FCS (GIBCO), stained with Türk's solution (Merck) and counted in Bürker chambers, or alternatively counted using the Sysmex KX-21 hematology analyzer.

Flow cytometry

FACS analysis of the myeloerythroid compartment in BM was performed as previously described[15,25]. Antibodies used are listed in the supplementary table 1. To evaluate lineage distribution between myeloid, B and T cells in the peripheral blood, erythrocytes were removed by sedimentation with Dextran (2%, Sigma-Aldrich) and ACK lysis. Following the lysis of erythrocytes, cells were stained for surface markers**.** For cell cycle analyses, c-Kit-enriched BM cells were cultured for 72 hours and 0.5 x10^6 cells were stained for c-Kit. BD Cytofix/Cytoperm™ Fixation/Permeabilization Kit (BD Biosciences; 554714) was utilized for intracellular staining according to manufacture's instructions and DNA was stained with DAPI (Sigma-Aldrich). Experiments were performed using FACS Aria cell sorter (Becton Dickinson) and LSR II flow cytometer (Becton Dickinson), and analyzed using FlowJo software (Tree Star, v9.7.6).

Cell culture

c-Kit$^+$ cells were enriched using CD117 MicroBeads and MACS separation columns (Miltenyi), and cultured in StemSpan®SFEM medium (StemCell Technologies) supplemented with penicillin/streptomycin (GIBCO), mSCF (100 ng/mL, PeproTech), mIL-3 (10 ng/mL, PeproTech) and hEPO (2 U/mL, Janssen-Cilag) ±doxycycline (1 μg/mL; Sigma-Aldrich).

Expression analyses

Total RNA was isolated from cultured cells after 48 hours using the RNAeasy micro kit (Qiagen). cDNA was transcribed using SuperScript III reverse trancriptase (Life Technologies). Real-time PCR reactions were performed using pre-designed assays (Life Technologies) with the exception of *Rps19* that was quantified using the SYBR GreenER™ system (5'-GCAGAGGCTCTAAGAGTGTGG-3'; 5'-CCAGGTCTCTCTGTCCCTGA-3') according to manufacturer's instructions (Life Technologies, 11761-500).

Immunoblotting

Whole cell extracts were prepared by harvesting of cells directly into Laemmli sample buffer (Bio-Rad) followed by sheering of the chromatin using a needle and boiling of the extracts. Proteins were separated on ready-made SDS-PAGE gels (Life Technologies). Proteins on gels were transferred to nitrocellulose membranes using a Trans-Blot Turbo machine (Bio-Rad). Equal loading of protein was verified by Ponceau S staining and confirmed by immunoblotting for β-actin. Blots were blocked in 5% milk in PBS for at least 20 min and subsequently incubated with the appropriate primary antibodies overnight at 4°C on a shaker. After three 5-minute washes with PBS, the blots were incubated with the appropriate secondary horse radish peroxidase conjugated antibody at room temperature for two hours followed by detection using the SuperSignal West Pico reagent (Thermo Scientific). Antibodies used are listed in the supplementary table 2. Immunoblots were quantified using the Image J software.

Statistical analyses

Student's *t* test was used to determine statistical significance, and two-tailed *P* values are shown. Cell culture and expression analysis-related *n* represents individual biological repeat experiments. A minimum of three biological replicate experiments was performed to justify the use of chosen statistical test.

RESULTS

Disruption of the 5S RNP-Mdm2 interaction improves the expansion of Rps19-deficient hematopoietic progenitor cells

To study the relevance of the 5S RNP-Mdm2-p53 pathway in DBA we took advantage of our mouse model for RPS19-deficient DBA[15]. This model contains an *Rps19*-targeting shRNA (shRNA-B) that is expressed by a doxycycline-responsive promoter located downstream of the *Collagen A1* gene, allowing for an inducible and dose-dependent Rps19 downregulation (Figure 1A). All experimental animals were bred homozygous for the *M2-rtTA* at the *Rosa26*

187 locus. Administration of doxycycline to the shRNA-B mice results in a severe
188 erythroid phenotype that is reversed in the p53-deficient background[15].
189 Importantly, the hematopoietic phenotype in these mice is specific to Rps19
190 downregulation as it can be cured by enforced expression of *RPS19*[15,26]. We
191 intercrossed the shRNA-B mice with the $Mdm2^{C305F}$ knock-in mice that have a
192 point mutation in the zinc finger domain of Mdm2, which prevents its binding to
193 5S RNP (Figure 1B)[23,24]. As a consequence these mice present with an
194 attenuated p53 response upon ribosome biogenesis stress, but retain a normal
195 response to DNA damage[23]. As a working model, we hypothesized that if the p53
196 response in Rps19-deficient mice is mediated through the 5S RNP-Mdm2
197 interaction, the $Mdm2^{C305F}$ background should reverse the p53 activity and
198 subsequently improve the erythroid phenotype of these mice (Supplementary
199 figure 1). To confirm that the $Mdm2^{C305F}$ background had no effect on the *Rps19*
200 knockdown efficiency in our model system, we quantified the expression of
201 *Rps19* in cultures initiated with c-Kit-enriched hematopoietic progenitor cells from
202 heterozygous (B/+; 1 shRNA-B allele) and homozygous (B/B; 2 shRNA-B alleles)
203 shRNA-B mice. After 48 hours of doxycycline treatment, the B/+ and B/B cells
204 showed on average 45% and 75% reduction in *Rps19* expression, respectively,
205 and $Mdm2^{C305F}$ had no significant impact on the *Rps19* knockdown efficiency
206 (Figure 1C).
207 We have previously shown that induction of Rps19 deficiency impairs expansion
208 of hematopoietic progenitor cells[15]. Therefore, we first assessed the effect of
209 $Mdm2^{C305F}$ on the expansion of Rps19-deficient hematopoietic progenitor cells *in*
210 *vitro*. After 5 days, the uninduced control cultures with wild-type Mdm2 or
211 homozygous $Mdm2^{C305F}$ showed no difference in cell number ($5.04\pm0.91 \times 10^6$
212 and $5.04\pm0.83 \times 10^6$, respectively) (Figure 1D). In contrast, the doxycycline-
213 treated B/+ cultures with wild-type Mdm2 showed a significant reduction in cell
214 number ($2.99\pm0.82 \times 10^6$), and this was improved in a dose-dependent manner in
215 the heterozygous and homozygous $Mdm2^{C305F}$ background ($3.87\pm0.56 \times 10^6$ and
216 $4.68\pm0.93 \times 10^6$, respectively) (Figure 1D). The B/B cultures with wild-type Mdm2
217 failed to expand and had $0.32\pm0.12 \times 10^6$ cells after 4 days of culture, while the

heterozygous and homozygous Mdm2^{C305F} background resulted in significant, partial restoration of cell numbers (0.63±0.21 x10^6 and 0.99±0.14 x10^6, respectively) (Figure 1D).

In order to assess whether the reduced expansion of Rps19-deficient hematopoietic progenitors was mainly due to altered proliferation or apoptosis, we performed DNA content analysis of the B/B cultures using flow cytometry. Induction of Rps19 deficiency resulted in a dramatic increase in the frequency of apoptotic cells as indicated by accumulation of these cells in the sub-G1 cell cycle phase that corresponds to cells with hypodiploid DNA content (Figure 1E). Furthermore, and similar to our previous study demonstrating a delay in G1/S transition in Rps19-deficient erythroblasts *in vivo*[15], following the exclusion of apoptotic cells in the sub-G1 fraction from our analysis we observed a significant accumulation of Rps19-deficient cells in the G1 cell cycle phase (Figure 1E). While the heterozygous Mdm2^{C305F} background resulted in a partial rescue of both viability and cell cycle progression, the extent of rescue in the homozygous Mdm2^{C305F} background was close to complete (Figure 1E).

5S RNP-Mdm2 interaction underlies the p53 activation in Rps19-deficient hematopoietic progenitor cells regardless of the level of Rps19 downregulation

Next, we assessed the impact of Rps19 deficiency on p53 response by quantifying the expression of p53 transcriptional target genes (*Cdkn1a*, *Ptp4a3*, *Zmat3*, *Bax*, *Ccng1* and *Phlda3*)[15] in c-Kit-enriched hematopoietic progenitor cells. Comparison of uninduced cultures with wild-type or homozygous Mdm2^{C305F} background revealed no differences in the expression of the p53 target genes with the exception of *Zmat3* that was found to be significantly upregulated by Mdm2^{C305F} (Figure 2A). However, the induction of Rps19 deficiency triggered a profound p53 response that was dependent on the level of Rps19 deficiency. For instance, the fold increase in expression of *Cdkn1a (p21)* in B/+ and B/B cultures was 1.8 and 4, respectively. Mdm2^{C305F} significantly

reduced the expression of p53 target genes in a dose-dependent manner regardless of the level of Rps19 downregulation (Figure 2A).

Analysis of the doxycycline-treated B/B cells revealed a robust downregulation of Rps19 protein (Figure 2B and 2C). Furthermore, correlating with the activation of p53 transcriptional response, doxycycline-treated B/B cells with wild-type Mdm2 showed accumulation of the p53 protein as well as its transcriptional target Mdm2 (Figure 2B and 2C). Remarkably, a homozygous $Mdm2^{C305F}$ background reversed the accumulation of p53. Finally, in agreement with previous studies[27,28], Rps19-deficient cells showed a decrease in the total level of Rps6, but the pool of phosphorylated Rps6 was increased (Figure 2C). Interestingly, $Mdm2^{C305F}$ had no effect on the phosphorylation of Rps6.

Disruption of the 5S RNP-Mdm2 interaction significantly improves the erythroid defect in Rps19-deficient mice

To study the physiological relevance of our *in vitro* findings we transplanted BM from the B/B mice into lethally irradiated wild-type recipients (Figure 3A). We chose this experimental strategy since we have previously shown that doxycycline treatment of the B/B mice results in *Rps19* haploinsufficiency and the resulting hematopoietic phenotype is autonomous to the blood system[15]. Furthermore, this strategy allowed us to monitor the impact of $Mdm2^{C305F}$ on the hematopoietic recovery from transplantation before the onset of Rps19 deficiency. To assess whether $Mdm2^{C305F}$ had an effect on hematopoiesis *per se*, we analyzed the peripheral blood one month after transplantation. No obvious differences in hematological parameters were observed between the recipients transplanted with control or heterozygous $Mdm2^{C305F}$ BM (Figure 3B, Supplementary table 3). By contrast, when compared to mice with wild-type Mdm2, the recipients with homozygous $Mdm2^{C305F}$ BM showed a significant decrease in the number of erythrocytes (93 % of the recipients with wild-type Mdm2), hemoglobin concentration (95 % of the recipients with wild-type Mdm2), number of white blood cells (74 % of the recipients with wild-type Mdm2), and

macrocytosis (Figure 3B). No differences in the number of reticulocytes were observed (Supplementary table 3).

Next the recipient mice were administered doxycycline for two weeks in order to induce Rps19 deficiency. The onset of Rps19 deficiency leads to a rapid reduction in blood cellularity that is rescued in the p53-null background[15]. As Rps19-deficient mice are partly able to compensate for the erythroid defect caused by the induction of Rps19 deficiency, monitoring the blood and BM cellularity during the first weeks of doxycycline administration provides a valid model to assess the effect of $Mdm2^{C305F}$ on the erythroid recovery of Rps19-deficient mice[25]. Doxycycline administration to the recipients transplanted with B/B BM cells resulted in a robust reduction in the number of erythrocytes (58 % of control), reticulocytes (67 % of control), and hemoglobin concentration (59 % of control) (Figure 3C, Supplementary table 4). Heterozygous and homozygous $Mdm2^{C305F}$ background led to a significant increase in all erythroid parameters, demonstrating the physiological relevance of the 5S RNP-Mdm2-p53 pathway for the erythroid defect in Rps19-deficient mice (Figure 3C, Supplementary table 4). In addition to improved erythropoiesis, the recipients with $Mdm2^{C305F}$ showed an increase in the number of platelets and total BM cellularity, further demonstrating the more pronounced hematological recovery after induction of Rps19 deficiency in these mice (Figure 3C-D). Finally, despite the reduction in white blood cells prior to doxycycline administration by $Mdm2^{C305F}$ (Figure 3B), $Mdm2^{C305F}$ had no negative effect on white blood cell number in the recipients with Rps19-deficient BM (Figure 3C).

$Mdm2^{C305F}$ knock-in mice show selective defect in erythropoiesis

Given the negative impact of $Mdm2^{C305F}$ *per se* on the hematopoietic recovery after transplantation (Figure 3B), we decided to characterize the hematopoietic phenotype of the $Mdm2^{C305F}$ knock-in mice in more detail. Indeed, careful elucidation of the hematopoietic phenotype caused by $Mdm2^{C305F}$ is essential in order to estimate the significance of the 5S RNP-Mdm2-p53 pathway on Rps19-deficient erythropoiesis (Figure 3C). Peripheral blood analysis revealed no

significant differences between control and heterozygous Mdm2^{C305F} mice (Figure 4A). However, similar to recipients transplanted with the homozygous Mdm2^{C305F} BM (Figure 3B), the homozygous Mdm2^{C305F} knock-in mice showed significant decrease in the number of erythrocytes that was associated with macrocytosis, and decrease in hemoglobin concentration (Figure 4A). In addition to the erythroid phenotype we observed an increase in the number of platelets (Figure 4A).

To gain further insights on the nature of the hematopoietic defect in the homozygous Mdm2^{C305F} knock-in mice we applied FACS strategies that allow for fractionation of HSCs, myeloerythroid progenitors and erythroid precursors in the BM[15,25] (Supplementary figure 2A and 2B). Correlating with the reduced number of erythrocytes in the peripheral blood, BM of the homozygous Mdm2^{C305F} mice showed a distinct reduction in the frequency of erythroid-committed preCFU-E (64 % of control) and CFU-E (57 % of control) progenitor cells, and more mature erythroblasts in otherwise normocellular BM (Figure 4B and 4C, and Supplementary figure 2C).

Although we observed no major differences in p53 response between uninduced (Rps19-proficient) wild-type and homozygous Mdm2^{C305F} cultures of c-kit-enriched hematopoietic stem and progenitor cells (Figure 2A), we wanted to confirm the impact of Mdm2^{C305F} on the p53 pathway in highly purified progenitor subpopulations. Given the strict correlation between the expression of p53 transcriptional target genes and the level of p53 protein (Figure 2A-C), we used the expression of p53 transcriptional targets as an indicator of p53 activity. Strikingly, quantification of the p53 transcriptional targets in freshly isolated immature (Lineage^{-}Sca-1^{+}c-Kit^{+}; LSK), myeloid-committed (preGM/GMP) and erythroid-committed (CFU-E) hematopoietic progenitor cells revealed a relatively selective and pronounced activation of the p53 signature in the erythroid-committed CFU-E progenitors of the homozygous Mdm2^{C305F} knock-in mice (Figure 4D). Corroborating these data, expression of two additional p53 transcriptional target genes *Phlda3* and *Bax* was increased on average 3.9 fold and 1.7 fold, respectively, in CFU-Es by Mdm2^{C305F} (Supplementary figure 3).

Mdm2^{C305F} ameliorates the functional decline of the hematopoietic system upon replicative stress

To study the impact of Mdm2^{C305F} on hematopoiesis upon stress, we transplanted lethally irradiated wild-type recipients with unfractionated control or Mdm2^{C305F} BM cells together with unfractionated congenic wild-type support BM (Figure 5A). In contrast to the primary Mdm2^{C305F} knock-in mice, the recipients of Mdm2^{C305F} BM cells developed a profound decrease in white blood cell reconstitution that appeared especially pronounced for the lymphoid lineages (Figure 5B). These results are in line with the significant decrease in the total number of white blood cells upon transplantation of homozygous Mdm2^{C305F} BM (Figure 3B), and demonstrate that the negative impact of Mdm2^{C305F} on hematopoiesis is not restricted to the erythroid lineage upon transplantation-mediated stress. As would be expected due to the competitive nature of the transplantation experiments, BM analysis of the recipients four to five months after transplantation revealed no differences in the total BM cellularity or in the frequency of HSCs and multipotent progenitor cells (MPPs) (Figure 5C). While the frequency of donor-derived MPPs was modestly decreased in the recipients with Mdm2^{C305F} BM, no difference was observed in the frequencies of donor-derived HSCs (Figure 5D).

To directly assess the effect of Mdm2^{C305F} on regenerative properties of HSCs, we FACS-sorted highly purified donor HSCs (CD45.2 LSK CD150+CD48-) from the control or homozygous Mdm2^{C305F} primary recipients, and transplanted them into lethally irradiated secondary recipients together with fresh unfractionated wild-type BM (Figure 5E). After five months, the recipients transplanted with control HSCs showed a robust myeloid reconstitution, while the reconstitution of the lymphoid lineages was low (Figure 5F). Surprisingly, the homozygous Mdm2^{C305F} HSCs gave rise to at least equivalent myeloid and lymphoid reconstitution compared to the control HSCs (Figure 5F). Therefore, when taking into account the significant negative impact mediated by Mdm^{C305F} in primary transplantations (Figure 5B), these data strongly indicate that Mdm2^{C305F} may

ameliorate the functional decline that normally associates with HSCs upon replicative stress.

DISCUSSION

Studies using animal models and primary human hematopoietic cells have suggested that the increased activation of p53 may be the underlying cause of the anemia in DBA[12-15]. Our current study confirms the prevailing hypothesis that the p53 activation upon Rps19 deficiency is dominantly mediated through the 5S RNP-Mdm2 interaction and demonstrates for the first time the physiological relevance of the 5S RNP-Mdm2-p53 pathway for the erythroid defect in DBA. Finally, our results suggest that the 5S RNP-Mdm2-p53 pathway may contribute to the replicative stress-associated functional decline of the hematopoietic system.

Our cell culture studies revealed an activation of the p53 pathway upon induction of Rps19 deficiency in c-Kit-enriched hematopoietic stem and progenitor cells and that the degree of the p53 response was strictly dependent on the level of Rps19 downregulation. $Mdm2^{C305F}$ caused a significant reduction in the level and activity of p53 regardless of the extent of Rps19 downregulation, demonstrating a dominant role of the 5S RNP-Mdm2 interaction for p53 activation upon Rps19 deficiency. Reduction of the p53 activity in Rps19-deficient hematopoietic stem and progenitor cells by $Mdm2^{C305F}$ normalized their viability and improved their proliferative capacity, resulting in significantly increased expansion of these cells *in vitro*. Importantly, reduction in p53 activity in cells with haploinsufficient expression of *Rps19*, a condition similar to DBA, led to a close to complete reversal of the expansion defect.

We and others have previously demonstrated that the hematopoietic phenotype upon Rps19 deficiency is reversed in the absence of p53[12,13,15]. However, the use of p53-deficient mice to study the relevance of p53 for the hematopoietic defect in DBA is problematic due to its additional role in restraining hematopoietic

stem and progenitor cell proliferation[29,30]. Indeed, increased influx of hematopoietic progenitor cells into the erythroid lineage in p53-deficient mice may mask the effect of p53-independent components that contribute to the erythroid defect in Rps19-deficient mice. Given that the Mdm2^{C305F} mice have wild-type p53, this model addresses more accurately the impact of p53 on Rps19-deficient hematopoiesis in absence of the physiological compensatory mechanisms present in the p53-deficient background. The significant improvement of the Rps19-deficient erythropoiesis by Mdm2^{C305F} clearly demonstrates the physiological and cell-autonomous relevance of the 5S RNP-Mdm2-p53 pathway for the disease phenotype *in vivo*. Interestingly, extent of the erythroid rescue by Mdm2^{C305F} was only partial, which was initially surprising given the robust improvement of the expansion defect of Rps19-deficient hematopoietic stem and progenitors *in vitro*. This finding can be explained in part by the subsequent identification of the selective erythroid defect caused by Mdm2^{C305F}. Indeed, the homozygous Mdm2^{C305F} knock-in mice showed a reduction in the frequency of erythroid-committed preCFU-E and CFU-E progenitor cells that was associated with a marked increase in the expression of p53 transcriptional target genes at these cellular stages. This erythroid-pronounced activation of the p53 signature was not detected in our cell culture experiments due to the low frequency of preCFU-E and CFU-E progenitors within the c-Kit-enriched hematopoietic stem and progenitor cells in the homozygous Mdm2^{C305F} mice. Finally, in contrast to the dose-dependent reversal of the p53 response by Mdm2^{C305F} *in vitro*, the heterozygous and homozygous Mdm2^{C305F} background resulted in comparable erythroid rescue in the Rps19-deficient recipients, further highlighting the negative impact of the Mdm2^{C305F} *per se* on erythropoiesis. Together with our earlier study locating the most severe erythroid defect in Rps19-deficient mice at the CFU-E stage[15], these data collectively indicate that both activation as well as disruption of the 5S RNP-Mdm2 interaction result in defective erythropoiesis at the level of CFU-E progenitor cell. Erythroid progenitor cells therefore appear especially sensitive to aberrations in p53 homeostasis mediated by the 5S RNP-Mdm2 interaction, with the 5S RNP-

Mdm2-p53 pathway representing a likely contributor to the complex pathogenesis of DBA, although the impact of additional and to date unidentified effects caused by inactivation of the Mdm2 zinc finger cannot be entirely ruled out.

In contrast to steady-state hematopoiesis, transplantation of $Mdm2^{C305F}$ BM revealed a significant reconstitution disadvantage compared to the wild-type cells, and this appeared especially pronounced for the lymphoid lineages. These data demonstrate that the defect caused by $Mdm2^{C305F}$ extends beyond the erythroid lineage upon hematopoietic stress. Despite an initial negative impact of $Mdm2^{C305F}$ on hematopoietic regeneration, serial transplantation of purified wild-type and homozygous $Mdm2^{C305F}$ HSCs resulted in comparable myeloid and lymphoid peripheral blood chimerism, suggesting that $Mdm2^{C305F}$ may provide HSCs with a reconstitution advantage over time. Since serial transplantation mimics many aspects of normal aging of the hematopoietic system[31], our data therefore implicate that the 5S RNP-Mdm2-p53 pathway may contribute to this process. Interestingly, aging-associated decrease in lymphopoiesis has been attributed to increased levels of the tumor suppressors p16 and p19Arf over time[32]. Given that the activation of p53 by p19Arf is at least partially dependent on the 5S RNP-Mdm2 interaction[22], we speculate that disruption of this pathway by $Mdm2^{C305F}$ in serially transplanted HSCs and their progeny could underlie the observed relative increase in their lymphoid reconstitution capacity.

Taken together, our study demonstrates the dominant role of the 5S RNP-Mdm2 interaction as a mediator of the p53 response upon Rps19 deficiency and provides the first physiological evidence that the 5S RNP-Mdm2-p53 pathway contributes to the anemia in DBA, and may also contribute to normal aging of the hematopoietic system.

ACKNOWLEDGEMENTS

This work was supported by The Swedish Children's Cancer Society (P.J., S.K.), The Crafoord Foundation (P.J.), The Gunnar Nilsson Cancer Foundation (D.B., P.J.), The Swedish Research Council (M.S.L., S.K.), The Swedish Cancer

Society (S.K.), Hemato-Linné grant (Swedish Research Council Linnaeus), The Tobias Prize awarded by The Royal Swedish Academy of Sciences financed by The Tobias Foundation (S.K.), and the EU project grants STEMEXPAND and PERSIST (S.K.).

CONFLICT OF INTEREST DISCLOSURE

The authors declare no conflict of interests.

CORRESPONDENCE

Stefan Karlsson, Molecular Medicine and Gene Therapy, BMC A12, 221 84, Lund, Sweden; email: stefan.karlsson@med.lu.se

Supplementary information is available at Leukemia's website.

REFERENCES

1. Willig TN, Niemeyer CM, Leblanc T, Tiemann C, Robert A, Budde J *et al*. Identification of new prognosis factors from the clinical and epidemiologic analysis of a registry of 229 Diamond-Blackfan anemia patients. DBA group of Société d'Hématologie et d'Immunologie Pédiatrique (SHIP), Gesellshaft für Pädiatrische Onkologie und Hämatologie (GPOH), and the European Society for Pediatric Hematology and Immunology (ESPHI). *Pediatr Res* 1999; 46: 553-561.

2. Lipton JM, Atsidaftos E, Zyskind I, Vlachos A. Improving clinical care and elucidating the pathophysiology of Diamond Blackfan anemia: an update from the Diamond Blackfan Anemia Registry. *Pediatr Blood Cancer* 2006; 46: 558-564.

3. Vlachos A, Rosenberg PS, Atsidaftos E, Alter BP, Lipton JM. Incidence of neoplasia in Diamond Blackfan anemia: a report from the Diamond Blackfan Anemia Registry. *Blood* 2012; 119: 3815-3819.

4. Draptchinskaia N, Gustavsson P, Andersson B, Pettersson M, Willig TN, Dianzani I *et al*. The gene encoding ribosomal protein S19 is mutated in Diamond-Blackfan anaemia. *Nat Genet* 1999; 21:169-175.

5. Gazda HT, Grabowska A, Merida-Long LB, Latawiec E, Schneider HE, Lipton JM *et al*. Ribosomal protein S24 gene is mutated in Diamond-Blackfan anemia. *Am J Hum Genet* 2006; 79: 1110-1118.

6. Cmejla R, Cmejlova J, Handrkova H, Petrak J, Pospisilova D. Ribosomal protein S17 gene (RPS17) is mutated in Diamond-Blackfan anemia. *Hum Mutat* 2007; 28: 1178-1182.

7. Farrar JE, Nater M, Caywood E, McDevitt MA, Kowalski J, Takemoto CM *et al*. Abnormalities of the large ribosomal subunit protein, Rpl35A, in diamond-blackfan anemia. *Blood* 2008; 112: 1582-1592.

8. Gazda HT, Sheen MR, Vlachos A, Choesmel V, O'Donohue MF, Schneider H *et al*. Ribosomal protein L5 and L11 mutations are associated with cleft palate and abnormal thumbs in Diamond-Blackfan anemia patients. *Am J Hum Genet* 2008; 83: 769-780.

9. Doherty L, Sheen MR, Vlachos A, Choesmel V, O'Donohue MF, Clinton C *et al*. Ribosomal protein genes RPS10 and RPS26 are commonly mutated in Diamond-Blackfan anemia. *Am J Hum Genet* 2010; 86: 222-228.

10. Gazda, HT, Preti M, Sheen MR, O'Donohue MF, Vlachos A, Davies SM *et al*. Frameshift mutation in p53 regulator RPL26 is associated with multiple physical abnormalities and a specific pre-ribosomal RNA processing defect in diamond-blackfan anemia. *Hum. Mutat* 2012; 33: 1037-1044.

11. Landowski M, O'Donohue MF, Buros C, Ghazvinian R, Montel-Lehry N, Vlachos A *et al*. Novel deletion of RPL15 identified by array-comparative genomic hybridization in Diamond-Blackfan anemia. *Hum Genet* 2013; 132: 1265-1274.

12. McGowan KA, Li JZ, Park CY, Beaudry V, Tabor HK, Sabnis AJ *et al*. Ribosomal mutations cause p53-mediated dark skin and pleiotropic effects. *Nat Genet* 2008; 40: 963-970.

13. Danilova N, Sakamoto KM, Lin S. Ribosomal protein S19 deficiency in zebrafish leads to developmental abnormalities and defective erythropoiesis through activation of p53 protein family. *Blood* 2008; 112: 5228-5237.

14. Dutt S, Narla A, Lin K, Mulally A, Abayasekara N, Megerdichian C *et al*. Haploinsufficiency for ribosomal protein genes causes selective activation of p53 in human erythroid progenitor cells. *Blood* 2011; 117: 2567-2576.

15. Jaako P, Flygare J, Olsson K, Quere R, Ehinger M, Henson A *et al*. Mice with ribosomal protein S19 deficiency develop bone marrow failure and symptoms like patients with Diamond-Blackfan anemia. *Blood* 2011; 118: 6087-6096.

16. Vousden KH and Lu X. Live or let die: the cell's response to p53. *Nat Rev Cancer* 2002; 2: 594-604.

17. Vousden KH and Prives C. Blinded by the light: the growing complexity of p53. *Cell* 2009;137: 413-431.

18. Zhang Y and Lu H. Signaling to p53: ribosomal proteins find their way. *Cancer Cell* 2009; 16: 369-377.

19. Fumagalli S, Ivanenkov VV, Teng T, Thomas G. Suprainduction of p53 by disruption of 40S and 60S ribosome biogenesis leads to the activation of a novel G2/M checkpoint. *Genes Dev* 2012; 26:1028-1040.

20. Bursać S, Brdovcak MC, Pfannkuchen M, Orsolic I, Golomb L, Zhu Y *et al*. Mutual protection of ribosomal proteins L5 and L11 from degradation is essential for p53 activation upon ribosomal biogenesis stress. *PNAS* 2012; 109: 20467-20472.

21. Donati G, Peddigari S, Mercer CA, Thomas G. 5S ribosomal RNA is an essential component of a nascent ribosomal precursor complex that regulates the Hdm2-p53 checkpoint. *Cell Rep* 2013; 4: 87-98.

22. Sloan KE, Bohnsack MT, Watkins NJ. The 5S RNP couples p53 homeostasis to ribosome biogenesis and nucleolar stress. *Cell Rep* 2013; 5: 237-247.

23. Macias E, Jin A, Deisenroth C, Bhat K, Mao H, Lindström MS *et al*. An ARF-independent c-MYC-activated tumor suppressor pathway mediated by ribosomal protein-Mdm2 interaction. *Cancer Cell* 2010; 18: 231-243.

554 24. Lindstrom MS, Jin A, Deisenroth C, White Wolf G, Zhang Y. Cancer-
555 associated mutations in the MDM2 zinc finger domain disrupt ribosomal protein
556 interaction and attenuate MDM2-induced p53 degradation. *Mol Cell Biol* 2007;
557 27: 1056-1068.
558 25. Jaako P, Debnath S, Olsson K, Bryder D, Flygare J, Karlsson S. Dietary L-
559 leucine improves the anemia in a mouse model for Diamond-Blackfan anemia.
560 *Blood* 2012; 120: 2225-2228.
561 26. Jaako P, Debnath S, Olsson K, Modlich U, Rothe M, Schambach A *et al*.
562 Gene therapy cures the anemia and lethal bone marrow failure in a mouse model
563 for RPS19-deficient Diamond-Blackfan anemia. *Haematologica* 2014; 99: 1792-
564 1798.
565 27. Payne EM, Virgilio M, Narla A, Sun H, Levine M, Paw BH *et al*. L-Leucine
566 improves the anemia and developmental defects associated with Diamond-
567 Blackfan anemia and del(5q) MDS by activating the mTOR pathway. *Blood* 2012;
568 120: 2214-2224.
569 28. Idol RA, Robledo S, Du HY, Crimmins DL, Wilson DB, Ladenson JH *et al*.
570 Cells depleted for RPS19, a protein associated with Diamond Blackfan Anemia,
571 show defects in 18S ribosomal RNA synthesis and small ribosomal subunit
572 production. *Blood Cells Mol Dis* 2007; 39: 35-43.
573 29. TeKippe M, Harrison DE, Chen J. Expansion of hematopoietic stem cell
574 phenotype and activity in Trp53-null mice. *Exp Hematol* 2003; 31: 521-527.
575 30. Liu Y, Elf SE, Miyata Y, Sashida G, Liu Y, Huang G *et al*. p53 regulates
576 hematopoietic stem cell quiescence. *Cell Stem Cell* 2009; 4: 37-48.
577 31. Dykstra B, Olthof S, Schreuder J, Ritsema M, de Haan G. Clonal analysis
578 reveals multiple functional defects of aged murine hematopoietic stem cells. *J*
579 *Exp Med* 2011; 208: 2691-2703.
580 32. Signer RA, Montecine-Rodriquez E, Witte ON, Dorshkind K. Aging and
581 cancer resistance in lymphoid progenitors are linked processes conferred by
582 p16Ink4a and Arf. *Genes Dev* 2008; 22: 3115-3120.
583
584

FIGURE LEGENDS

Figure 1. Mdm2^{C305F} improves the expansion of Rps19-deficient hematopoietic progenitors *in vitro.* (A) Schematic overview of the transgenic Rps19 knockdown mouse model. This model contains an *Rps19*-targeting shRNA (shRNA-B) under the control of doxycycline-regulatable control element downstream of the *Collagen A1* gene, and constitutively active M2 reverse tetracycline transactivator (M2-rtTA) under the endogenous *Rosa26*[15]. (B) Schematic overview of the Mdm2^{C305F} knock-in mouse model. This model has a missense mutation in the central zinc finger domain of Mdm2 that disrupts its binding to the 5S RNP[23]. (C) Quantitative real-time PCR analysis of *Rps19* mRNA levels in cultures initiated with c-Kit-enriched BM cells isolated from heterozygous [B/+] and homozygous [B/B] shRNA-B mice. Samples for RNA extraction were collected after 48 hours (n= 6 for the groups without doxycycline; n= 3 for the groups with doxycycline). (D) Expansion of 0.5 x10^6 c-Kit-enriched BM cells in cultures (n= 6 for the groups without doxycycline; n= 4 for the groups with doxycycline). (E) Cell cycle analysis of c-Kit-enriched BM cells from in cultures. DNA content analysis was performed after 72 hours on c-Kit+ cells (n= 3 per group). Dean-Jett-Fox model was used to calculate percentages of cells in G0/G1, S, and G2/M phases (shown in brown). Data are presented as mean± standard deviation.

Figure 2. 5S RNP-Mdm2 interaction underlies the p53 activation in Rps19-deficient hematopoietic progenitor cells. (A) Quantitative real-time PCR analysis of previously identified p53 transcriptional target genes[15] in cultures initiated with c-Kit-enriched BM cells. Samples for RNA extraction were collected after 48 hours (n= 5 for the groups without doxycycline; n= 3 for the groups with doxycycline). (B) Representative immunoblots of Mdm2, p53 and Rps19 of cultures initiated with c-Kit-enriched B/B BM cells. Samples were collected after 48 hours. (C) Densitometry analysis of p53 and Rps19 protein shown in (B) (n= 3). (D) Representative immunoblots of Rps6 and p-Rps6 of cultures initiated with

c-Kit-enriched B/B BM cells. Samples were collected after 48 hours. Data are presented as mean± standard deviation.

Figure 3. Mdm2^{C305F} ameliorates the anemia in Rps19-deficient mice. (A) Experimental strategy to assess the effect of Mdm2^{C305F} on Rps19-proficient hematopoietic recovery following transplantation and on Rps19-deficient hematopoiesis. One million uninduced unfractionated BM cells were transplanted in 300 μL PBS into the tail vain of lethally irradiated (900 cGy) wild-type recipients. (B) Erythrocyte number, hemoglobin concentration, mean corpuscular volume (MCV), white blood cell and platelet numbers before the administration of doxycycline (n= 25, 24 and 33 for the [B/B; +/+], [B/B; C305F/+] and [B/B; C305F/C305F] groups, respectively). (C) Erythrocyte number, hemoglobin concentration, MCV, reticulocyte, white blood cell and platelet numbers two weeks after doxycycline administration (n= 28, 20, 19 and 19 for the [+/+; +/+], [B/B; +/+], [B/B; C305F/+] and [B/B; C305F/C305F] groups, respectively). (D) BM cellularity two weeks after doxycycline administration (n= 27, 18, 18 and 17 for the [+/+; +/+], [B/B; +/+], [B/B; C305F/+] and [B/B; C305F/C305F] groups, respectively). Data are presented as mean± standard deviation.

Figure 4. Mdm2^{C305F} knock-in mice show selective defect in erythropoiesis. (A) Erythrocyte number, hemoglobin concentration, mean corpuscular volume (MCV), platelet number and white blood cell number in primary Mdm2^{C305F} knock-in mice (n= 10, 16 and 9 for the [+/+], [C305F/+] and [C305F/C305F] groups, respectively). (B) Bone marrow cellularity (n= 8 per group). (C) Frequencies of erythroid committed preCFU-E and CFU-E progenitor cells, and erythroblasts in the BM of primary Mdm2^{C305F} knock-in mice (n= 8 per group). (D) Quantitative real-time PCR analysis of previously identified p53 transcriptional target genes[15] in freshly isolated LSK, preGM/GMP and CFU-E progenitor populations (n= 4 per group). Data are presented as mean± standard deviation. EB=erythroblast.

Figure 5. Mdm2^{C305F} ameliorates the functional decline of the hematopoietic system upon replicative stress. (A) Experimental strategy to assess the impact of Mdm2^{C305F} on transplantation-mediated hematopoietic stress. 0.66 million unfractionated donor BM cells were transplanted together with 0.33 million unfractionated support BM cells in 300 μL PBS into the tail vain of lethally irradiated (900 cGy) wild-type recipients. (B) Myeloid (CD11b+), B cell (CD19+) and T cell (CD3+) donor reconstitution in primary recipients one and four months after transplantation (n= 26, 14 and 26 for the [+/+], [C305F/+] and [C305F/C305F] groups, respectively). (C) Bone marrow cellularity and (D) frequencies of total and donor-derived HSCs (CD45.2 LSK CD150+ CD48-) and multipotent progenitor (MPP; CD45.2 LSK CD150- CD48-) cells in primary recipients four to five months after transplantation (n= 27, 13 and 26 for the [+/+], [C305F/+] and [C305F/C305F] groups, respectively). (E) Experimental strategy to assess the impact of Mdm2^{C305F} on regenerative properties of HSCs. BM from primary recipients were pooled per genotype and 375 FACS-sorted donor HSCs (CD45.2 LSK CD150+ CD48-) were transplanted together with 0.4 million fresh unfractionated support BM cells in 300 μL PBS into the tail vain of lethally irradiated (900 cGy) wild-type recipients. (F) Myeloid (CD11b+), B cell (CD19+) and T cell (CD3+) donor reconstitution in secondary recipients five months after transplantation (n= 11 per group and represents the average of two biological experiments). Data are presented as mean± standard deviation.

Figure 1

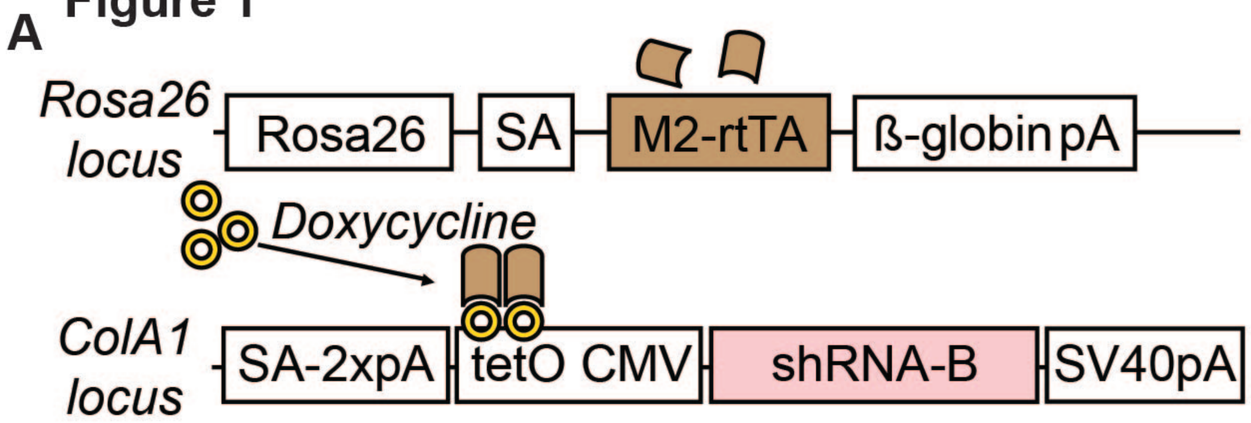

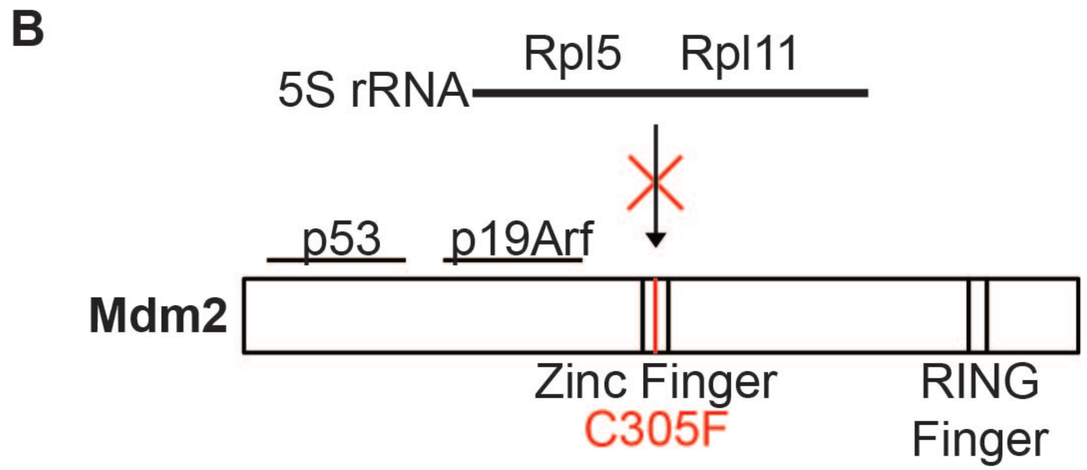

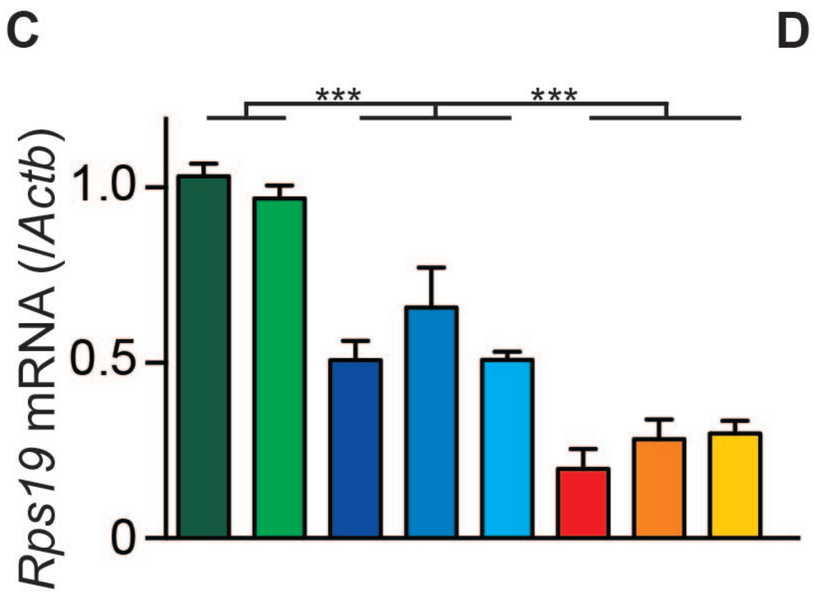

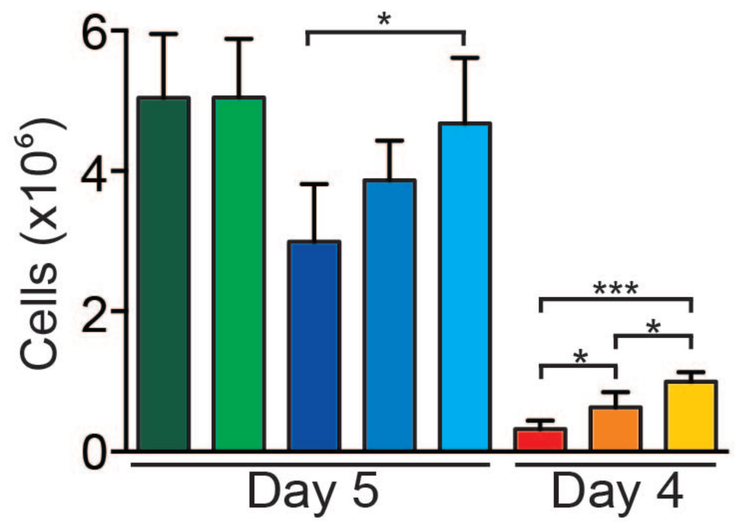

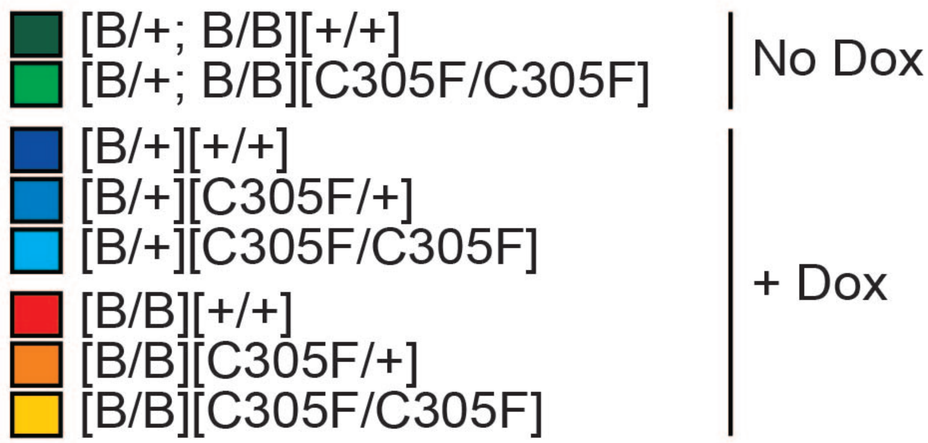

*P <0.05
**P <0.01
***P <0.001

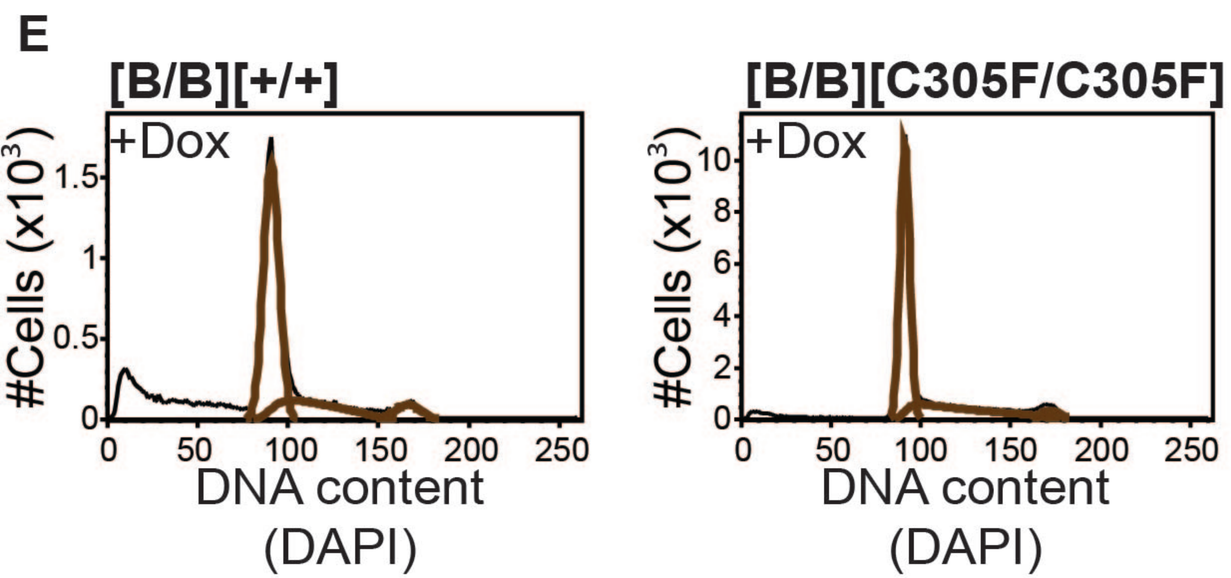

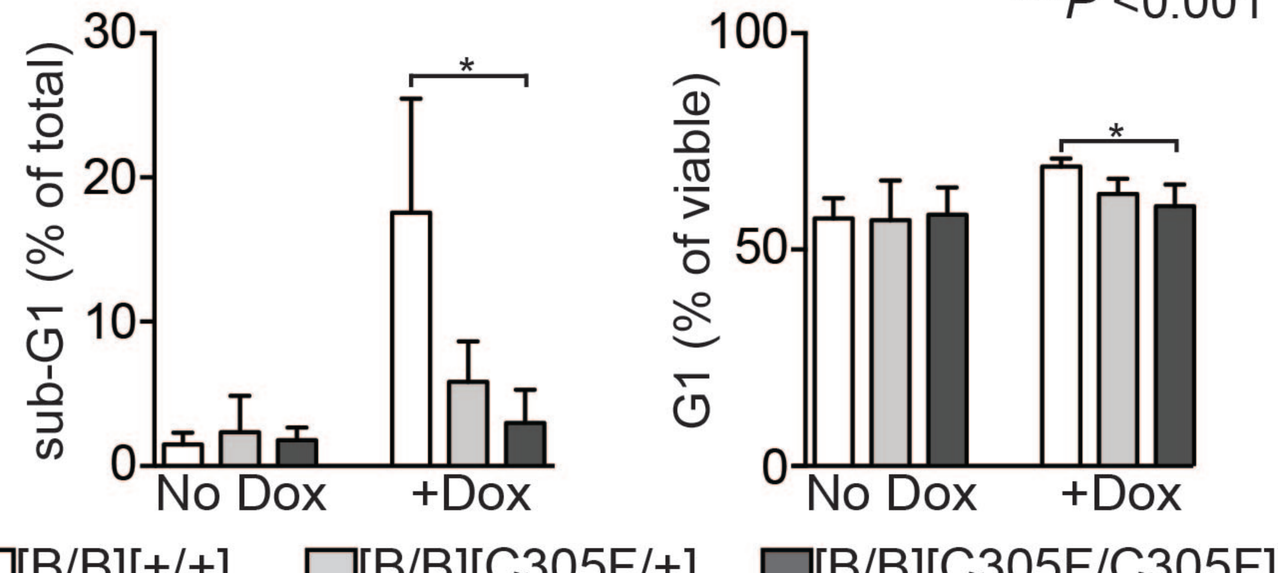

Figure 2

A

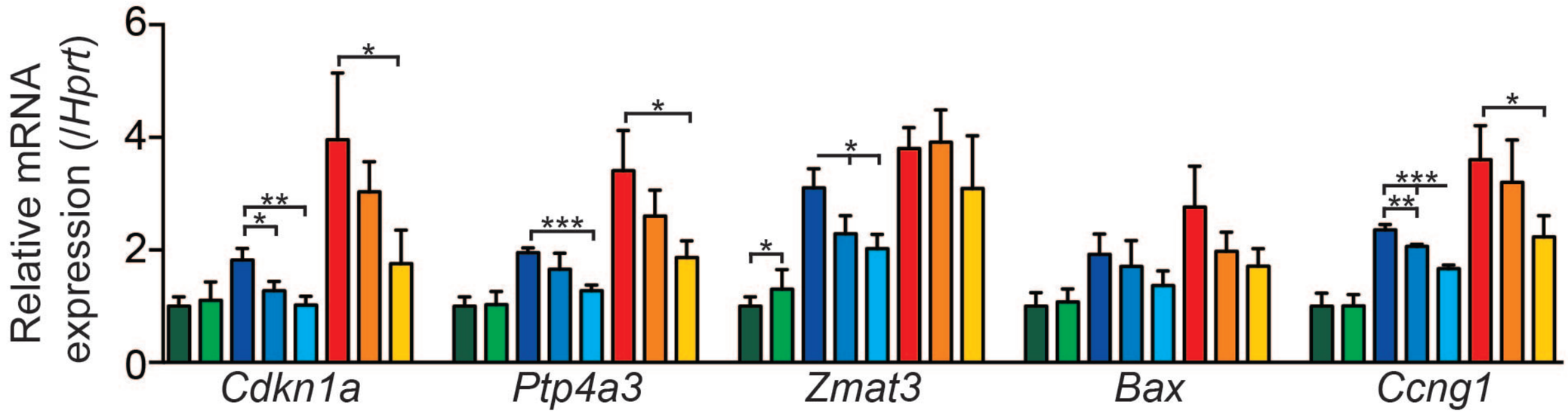

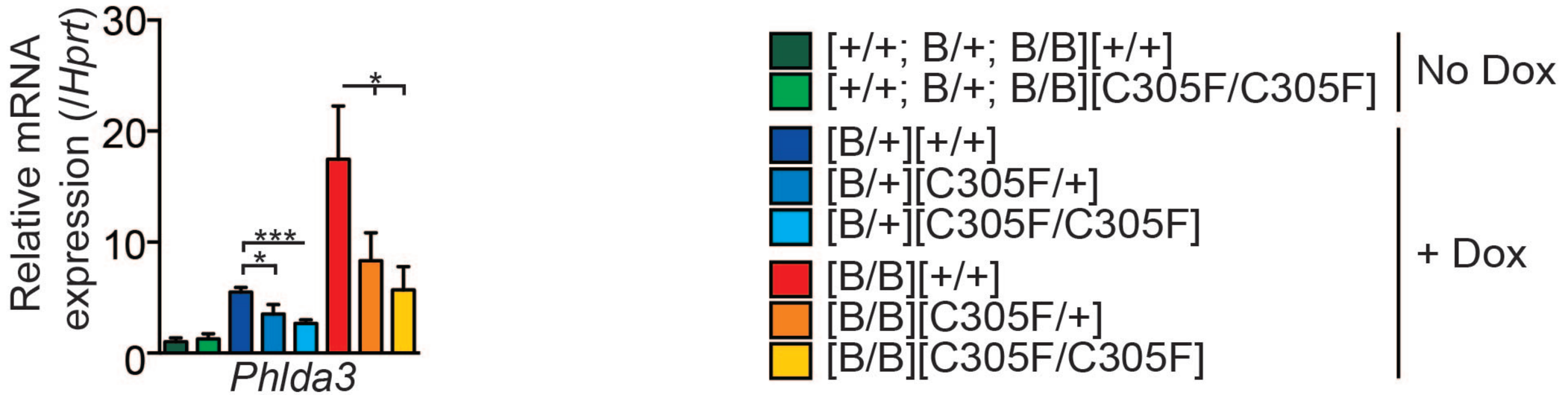

B

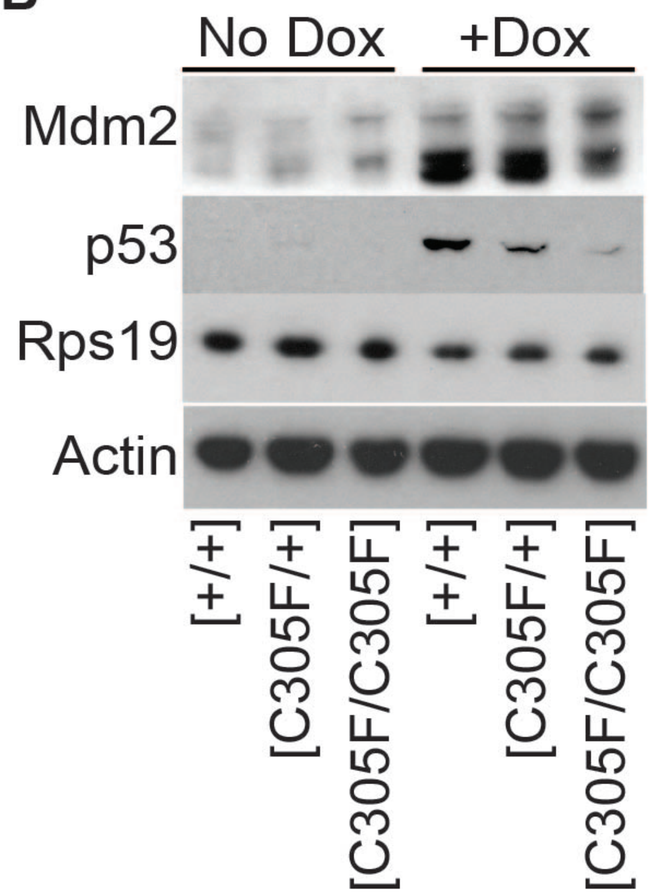

C

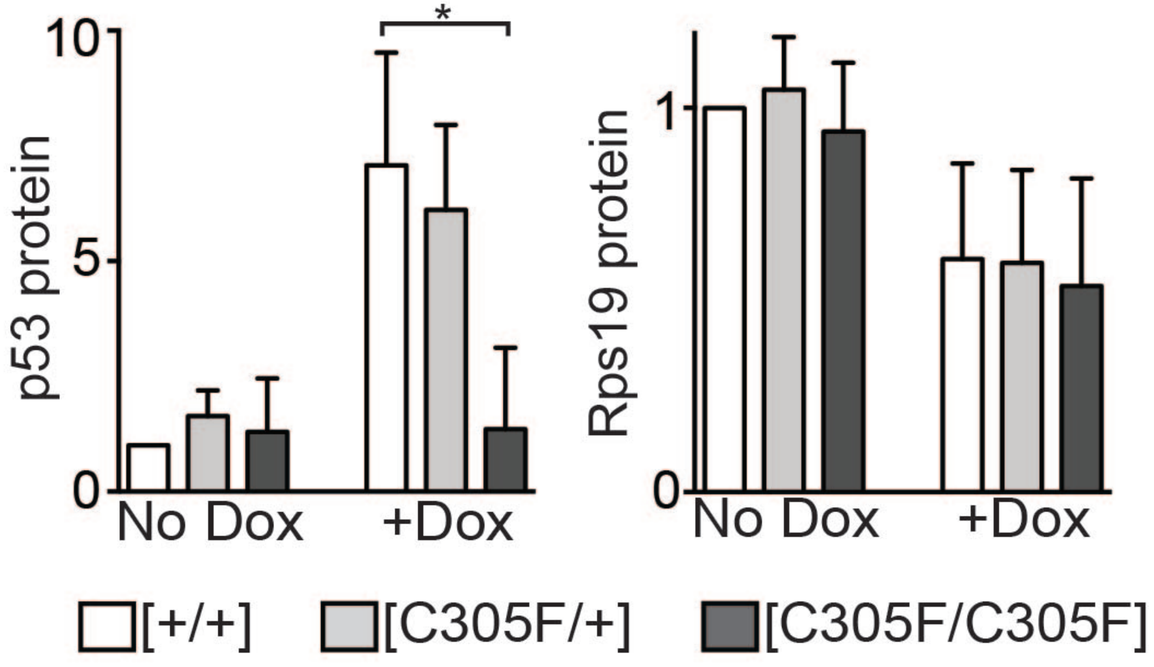

D

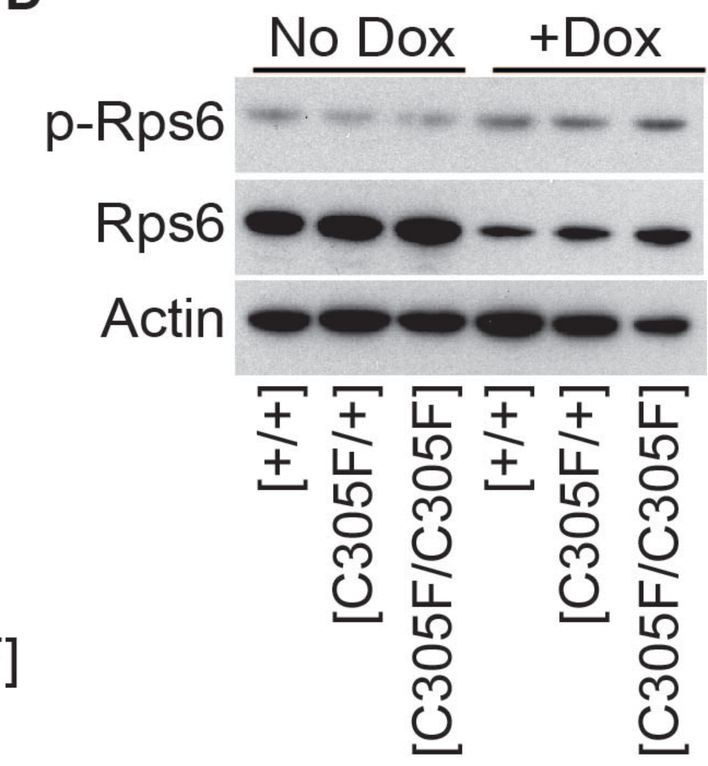

Figure 3

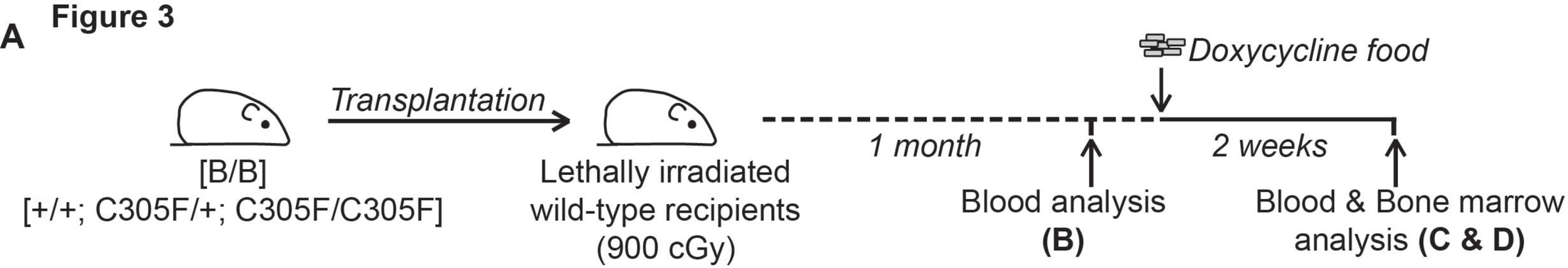
A
Transplantation
[B/B]
[+/+; C305F/+; C305F/C305F]
Lethally irradiated
wild-type recipients
(900 cGy)
Doxycycline food
1 month
2 weeks
Blood analysis
(B)
Blood & Bone marrow
analysis (C & D)
B
Erythrocytes (x10^12/L)
Hemoglobin [g/L]
MCV [fL]
White blood cells (x10^9/L)
Platelets (x10^9/L)
Uninduced
C
Erythrocytes (x10^12/L)
Hemoglobin [g/L]
MCV [fL]
Reticulocytes (x10^9/L)
White blood cells (x10^9/L)
Platelets (x10^9/L)
Bone marrow cellularity (x10^6)
D
+Doxycycline
*P <0.05
**P <0.01
***P <0.001
[+/+; +/+]
[B/B; +/+]
[B/B; C305F/+]
[B/B; C305F/C305F]

Figure 4

A

Erythrocytes (x10^{12}/L)

Hemoglobin [g/L]

MCV [fL]

Platelets (x10^{9}/L)

White blood cells (x10^{9}/L)

B

BM cellularity (x10^{6})

C

Frequency in BM (%)

preCFU-E

CFU-E

EB Fr. I

EB Fr. II

EB Fr. III

p=0.05

D

LSK

preGM/GMP

CFU-E

Relative epxression (/Hprt)

Cdkn1a

Ptp4a3

Ccng1

Zmat3

[+/+]

[C305F/+]

[C305F/C305F]

*P <0.05
**P <0.01
***P <0.001

Figure 5

A

Transplantation

0.66x10⁶ BM (donor; CD45.2)

0.33x10⁶ BM (support; CD45.1)

[+/+; C305F/+; C305F/C305F]

Lethally irradiated wild-type recipients (CD45.1; 900 cGy)

1 month — Blood analysis **(B)**

4 months — Blood analysis **(B)**

BM analysis **(C-D)**

B

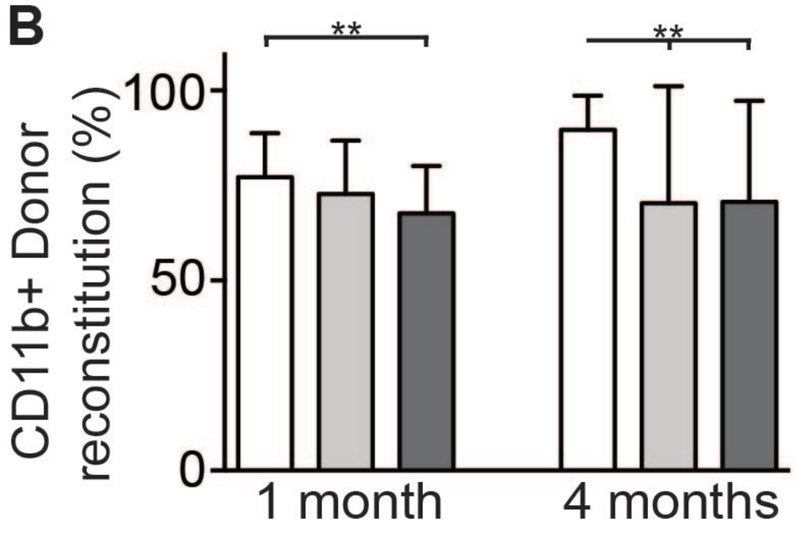

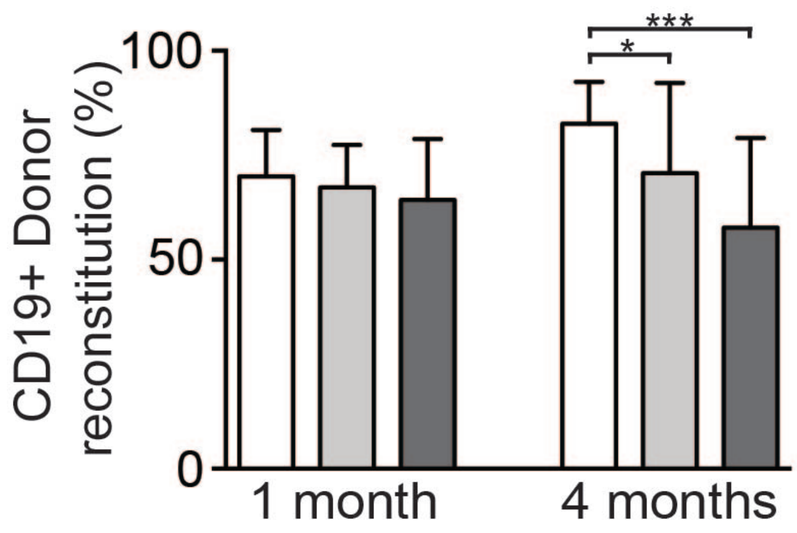

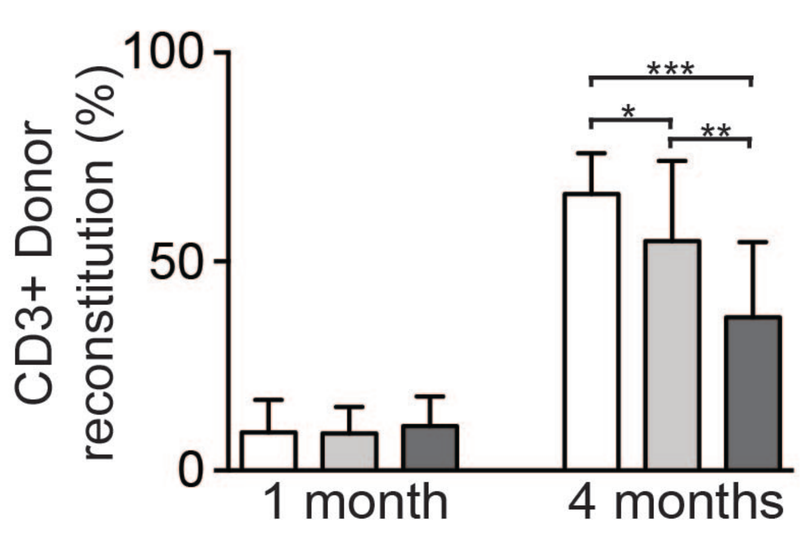

C

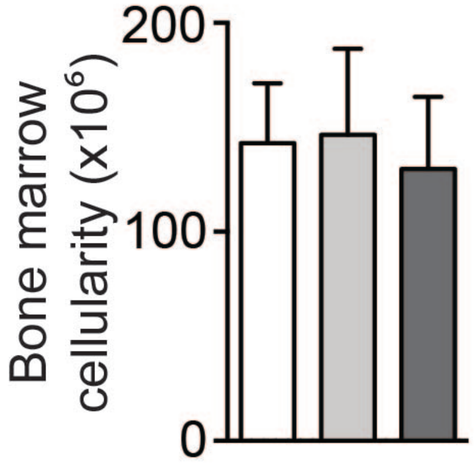

D

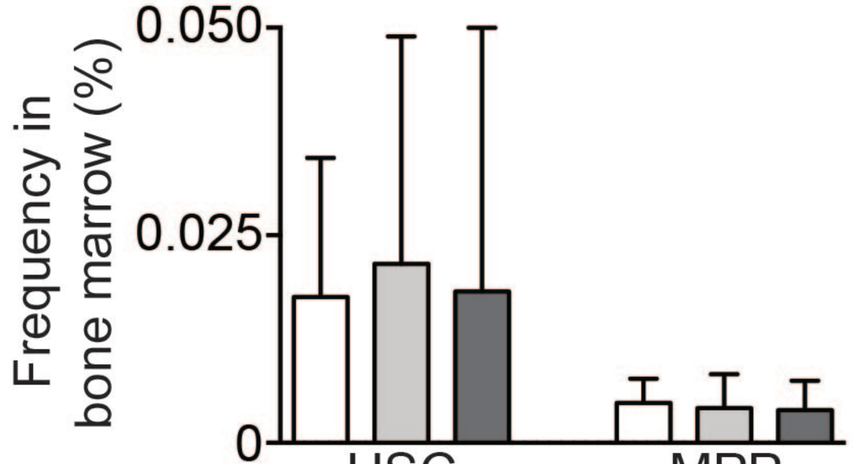

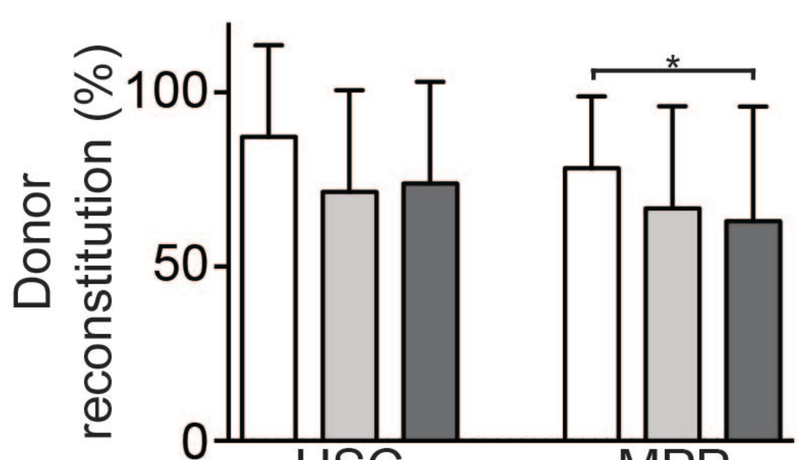

*P <0.05
**P <0.01
***P <0.001

[+/+] [C305F/+] [C305F/C305F]

E

2ary transplantation

375 HSCs (donor; CD45.2)

0.4x10⁶ BM (support; CD45.1)

[+/+; C305F/C305F]

Lethally irradiated wild-type recipients (CD45.1; 900 cGy)

F

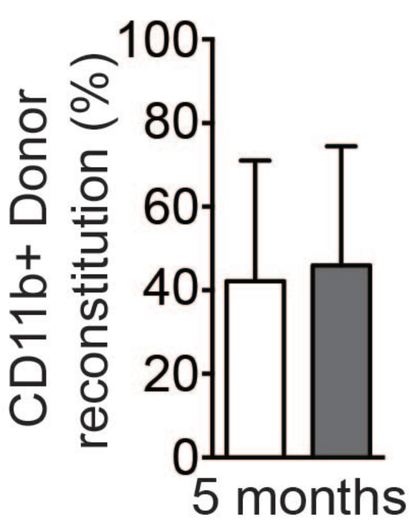

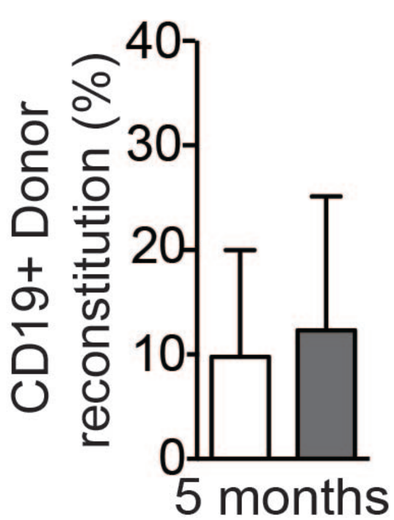

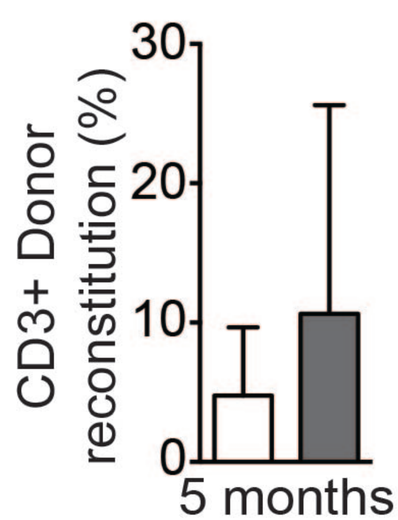

Supplementary table 1. List of antibodies and reagents used for flow cytometry.

	Fluorochrome	Cat#	Manufacturer
BM analysis:			
CD45.2	FITC	109806	Biolegend
CD71	FITC	113806	Biolegend
CD41	PE	12-0411-83	eBioscience
CD45.1	PE	110708	Biolegend
GR1	PE-Cy5 (Lineage)	108410	Biolegend
CD11b	PE-Cy5 (Lineage)	101210	Biolegend
B220	PE-Cy5 (Lineage)	103210	Biolegend
CD3	PE-Cy5 (Lineage)	100310	Biolegend
Ter119	PE-Cy7	25-5921-82	eBioscience
CD150	APC	115910	Biolegend
c-Kit	APC-eFluor780	47-1171-82	eBioscience
Endoglin	Biotin	120404	Biolegend
Sca-1	Pacific blue	122520	Biolegend
Streptavidin	QD605	Q10101MP	Life Technologies
Peripheral blood analysis:			
CD45.2	FITC	109806	Biolegend
CD45.1	PE	110708	Biolegend
CD19	PE-Cy7	25-0193-82	eBioscience
CD11b	APC	101212	Biolegend
CD3	Alexa Fluor® 700	100216	Biolegend
Cell cycle analysis:			
c-Kit	APC	105812	Biolegend

Supplementary table 2. List of antibodies used for immunoblotting experiments.

	Clone/Cat#	Manufacturer
β-actin	AC-15	Sigma-Aldrich
p53	sc-6243	Santa Cruz
MDM2	SMP14	Sigma-Aldrich
RPS19	ab57643	Abcam
RPS6	#2217	Cell Signaling Technologies
p-RPS6	#2215	Cell Signaling Technologies

Supplementary table 3. Erythrocyte number, hemoglobin concentration, mean corpuscular volume (MCV), reticulocyte, platelet number and white blood cell number before the administration of doxycycline.

	[B/B][+/+] *(n=25)*	**[B/B][C305F/+]** *(n=24)*	**[B/B][C305F/C305F]** *(n=33)*
Erythrocytes ($x10^{12}$ /L)	9.23±0.44 (100 %)	9.06±0.39 (98 %)	8.56±0.67 (93 %)
Hemoglobin (g/L)	136±8 (100 %)	133±6 (98 %)	129±8 (95 %)
MCV (fL)	48.1±0.3	47.7±0.7	49.5±3.0
Reticulocytes ($x10^9$/L)	257±71 (100 %)	255±39 (99 %)	267±76 (104 %)
Platelets ($x10^9$/L)	499±202 (100 %)	512±179 (103 %)	482±187 (97 %)
White blood cells ($x10^9$/L)	6.55±1.48 (100 %)	5.87±0.84 (90 %)	4.87±1.53 (74 %)

Supplementary table 4. Erythrocyte number, hemoglobin concentration, mean corpuscular volume, reticulocyte number, platelet number and white blood cell number 2 weeks after doxycycline administration.

	[+/+][+/+] *(n=28)*	**[B/B][+/+]** *(n=20)*	**[B/B][C305F/+]** *(n=19)*	**[B/B][C305F/C305F]** *(n=19)*
Erythrocytes (x10^{12} /L)	10.13±0.74 (100 %)	5.83±1.93 (58 %)	7.32±1.34 (72 %)	6.91±1.2 (68 %)
Hemoglobin (g/L)	145±11 (100 %)	85±29 (59 %)	106±21 (73 %)	105±19 (72 %)
MCV (fL)	47.8±1.3	48.3±1.9	48.2±2.1	51.2±1.1
Reticulocytes (x10^{9}/L)	202±59 (100 %)	135±127 (67 %)	203±124 (100 %)	231±88 (114 %)
Platelets (x10^{9}/L)	404±115 (100 %)	332±245 (82 %)	396±189 (98 %)	567±166 (140 %)
White blood cells (x10^{9}/L)	12±3 (100 %)	5.39±2.55 (45 %)	5.38±1.39 (45 %)	4.45±1.09 (37%)

Supplementary figure 1

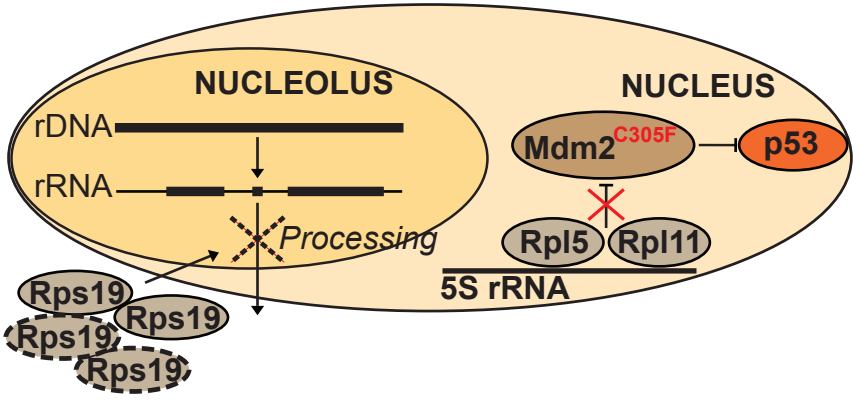

Supplementary figure 1. A working model of the effect of Mdm2^{C305F} on p53 activation upon Rps19 deficiency. Rps19 deficiency impairs the processing of rRNA (Jaako et al., Blood 2011), which leads to nuclear accumulation of the 5S ribonucleoprotein particle (5S RNP) that can bind to and inhibit Mdm2, resulting in the stabilization of p53. As Mdm2^{C305F} fails to bind the 5S RNP, it is expected to prevent the activation of p53 upon Rps19 deficiency.

Supplementary figure 2.

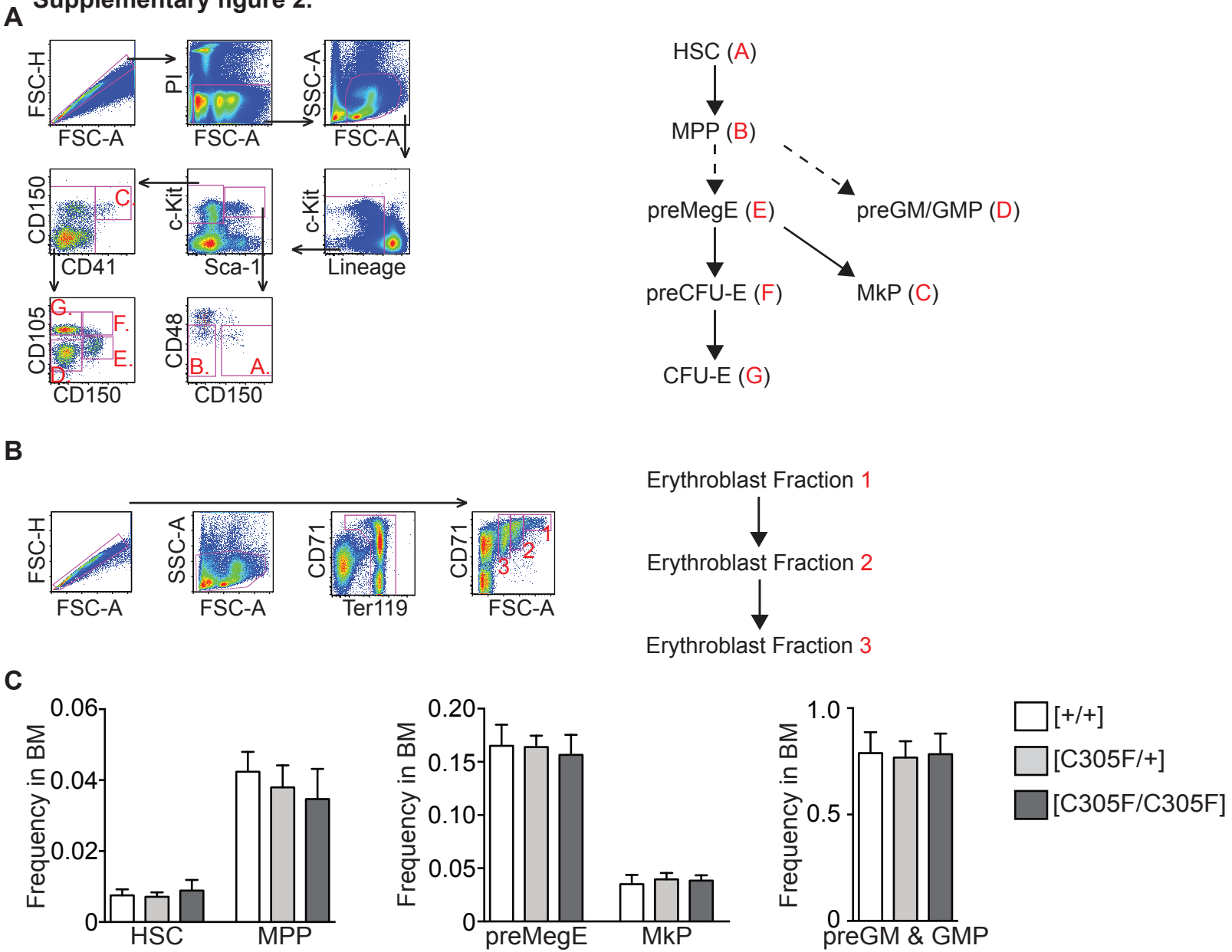

Supplementary figure 2. (A) FACS strategy allowing for the fractionation of HSCs and myeloerythroid progenitors. (B) FACS strategy allowing for the fractionation of erythroid precursors. (C) Frequency of HSCs, MPPs, preMegEs, MkPs and preGM/GMPs in the bone marrow (*n*=8 per genotype).

Supplementary figure 3

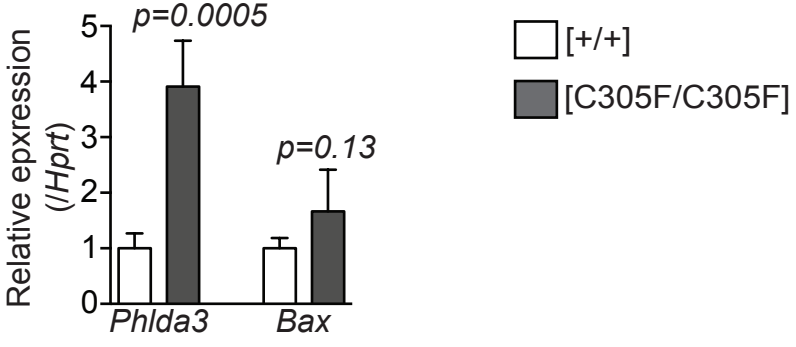

Supplementary figure 3. CFU-E erythroid progenitor cells from Mdm2^{C305F} knock-in mice show elevated expression of p53 transcriptional target genes Phlda3 and Bax. n=4 per genotype. Student's t test was used to determine statistical significance and two-tailed *P*-values are shown. Data are presented as mean± standard deviation.